

# ExploRLLM: Guiding Exploration in Reinforcement Learning with Large Language Models

Runyu Ma<sup>\*1</sup>, Jelle Luijckx<sup>\*1</sup>, Zlatan Ajanović<sup>2</sup>, and Jens Kober<sup>1</sup>

**Abstract**—In robot manipulation tasks with large observation and action spaces, reinforcement learning (RL) often suffers from low sample efficiency and uncertain convergence. As an alternative, foundation models have shown promise in zero-shot and few-shot applications. However, these models can be unreliable due to their limited reasoning and challenges in understanding physical and spatial contexts. This paper introduces ExploRLLM, a method that combines the commonsense reasoning of foundation models with the experiential learning capabilities of RL. We leverage the strengths of both paradigms by using foundation models to obtain a base policy, an efficient representation, and an exploration policy. A residual RL agent learns when and how to deviate from the base policy while its exploration is guided by the exploration policy. In table-top manipulation experiments, we demonstrate that ExploRLLM outperforms both baseline foundation model policies and baseline RL policies. Additionally, we show that this policy can be transferred to the real world without further training. Supplementary material is available at <https://explorllm.github.io>.

## I. INTRODUCTION

Foundation models (FMs) [1], which refer to models trained on large-scale data (e.g., Large Language Models or Vision-Language Models), have shown significant promise in robotics. Large Language Models (LLMs), such as GPT-4 [2], can generate commonsense-aware reasoning in various scenarios. For instance, LLMs have demonstrated zero-shot planning capabilities [3], breaking down complex tasks into detailed step-by-step plans without additional training. When integrated with Vision-Language Models (VLMs), LLMs leverage cross-domain knowledge for robot perception and planning in manipulation tasks [4]. This synergy allows for the extraction of environmental affordances and constraints, forming a foundation for subsequent robotic planning [5]. Despite the impressive results of FMs, unpredictable failures in LLM predictions can still lead to robotic errors, and LLMs generally do not learn from past experiences [6], [7].

Reinforcement Learning (RL) offers a powerful framework for learning decision-making and control policies through interaction with the environment [8]. However, RL struggles with the “curse of dimensionality,” where large observation and action spaces slow exploration and convergence. To address this, we propose combining FMs and RL, using FMs to guide the RL agent’s exploration. While actions generated by FMs may be sub-optimal or fail, they highlight

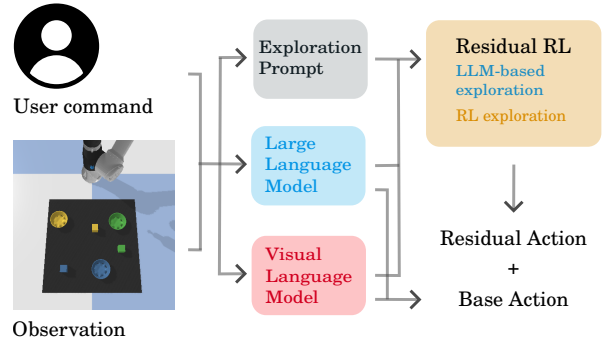


Fig. 1: Graphical overview of ExploRLLM.

meaningful regions in the action space for exploration. Traditional RL exploration strategies (e.g.,  $\epsilon$ -greedy, Boltzmann exploration [9]) are stochastic, focusing on exploration-exploitation trade-offs, but lack mechanisms to incorporate prior knowledge for faster convergence. We instead use LLMs as few-shot planners, generating actions that serve as exploration steps in RL, increasing the likelihood of successful states and gathering more relevant state-action pairs for off-policy RL agents.

Our method, ExploRLLM, improves performance by compensating for FMs’ sub-optimality and biases through RL, while FMs accelerate RL training by reducing observation spaces and guiding exploration. To summarize, our main contributions are: 1) We propose ExploRLLM, which employs an RL agent with a) residual action and observation spaces based on affordances identified by FMs and b) LLM-guided exploration. 2) We introduce a prompting method for LLM-based exploration using hierarchical language-model programs, leading to faster convergence. 3) We show that ExploRLLM outperforms policies derived solely from LLMs and VLMs and generalizes to unseen scenarios, tasks, and real-world settings without additional training.

## II. RELATED WORK

### A. Foundation Models for Planning in Robotics

Researchers have shown that LLMs can generate zero-shot or few-shot plans using reasoning capabilities [3], [10], which is crucial for high-level planning in robotics. These models facilitate task-level planning by integrating environmental groundings, such as affordance value scores [11] or feedback [12], with their language groundings. Furthermore, LLMs can generate robot-centric code programs as representations for both task-level [13] and skill-level planning [14].

<sup>\*</sup> Equal Contribution. <sup>1</sup> Cognitive Robotics, Delft University of Technology, The Netherlands (e-mail: {j.d.luijckx, j.kober}@tudelft.nl, r.ma-8@student.tudelft.nl). <sup>2</sup> RWTH Aachen University, Germany (e-mail: zlatan.ajanovic@ml.rwth-aachen.de).

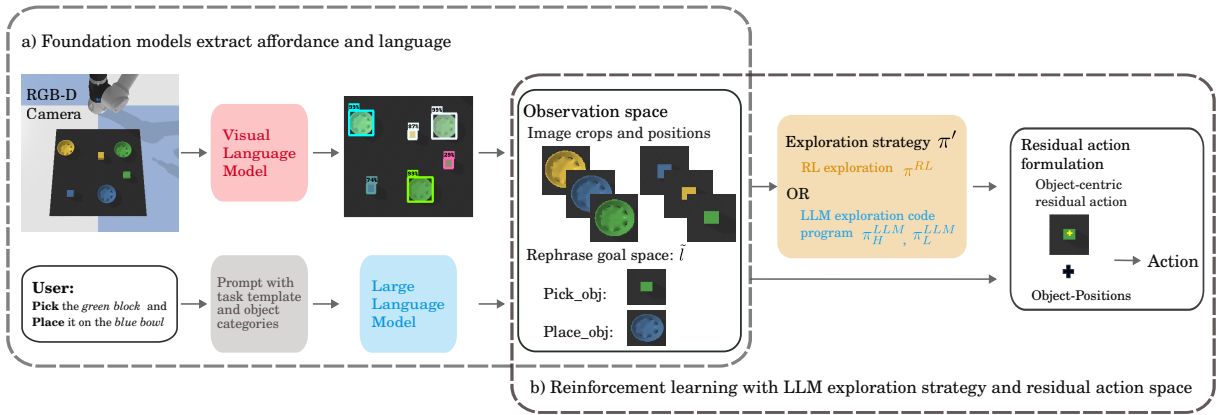


Fig. 2: Implementation structure of ExplorLLM for tabletop manipulation, combining the strengths of RL and FMs.

VLMs are increasingly integrated into robotics as a perception module of environmental context. The integration of knowledge from LLMs and VLMs facilitates the creation of perception-planning pipelines [4] and the construction of 3D value maps for zero-shot planning frameworks [5]. However, directly applying VLMs and LLMs to zero-shot tasks may not guarantee success or safety due to real-world uncertainty. In our research, we treat these actions as exploratory behaviors within an RL framework.

### B. Foundation Models and Reinforcement Learning

Incorporating FMs into RL frameworks has notably improved RL’s effectiveness. In [15], the authors have implemented LLMs as proxy reward functions, demonstrating their utility in RL. In the context of RL for robotics, LLMs are also capable of generating reward signals for robot actions by connecting commonsense reasoning with low-level actions [16], self-refinement [17] and evolutionary optimization over reward code to enable complex tasks such as dexterous manipulation [18]. Regarding exploration, authors in [19] reward RL agents toward human-meaningful intermediate behaviors by prompting an LLM. LLMs are also utilized as an intrinsic reward generator to guide exploration for long horizon manipulation tasks [20]. Contrary to these studies, our approach employs LLM-generated code policies to guide exploratory actions rather than focusing on reward shaping.

### III. PROBLEM FORMULATION

In this study, we focus on tabletop manipulation tasks to implement and evaluate our ExplorLLM method, as these tasks facilitate the creation of a base policy using FMs. We use a VLM for object detection and an LLM to identify the object to be manipulated from a command. Each manipulation task begins with a linguistically described goal, denoted by  $\tilde{l}$ . At each time step  $t$ , the agent receives an observation  $\mathbf{o}^t$ , consisting of an overhead RGB-D image and the state of the end-effector. Similar to existing methods (e.g., Transporter [21]), the action space involves a pick and a place primitive, denoted as  $\{\mathcal{P}_{\text{pick}}, \mathcal{P}_{\text{place}}\}$ , with each action parameterized by pick and place positions in a top-down view. We simplify this to a single motion primitive—either

pick or place. This simplification makes the RL challenge more tractable by eliminating the need to learn a feature representation for each primitive individually. The pick or place action is defined as a tuple containing the primitive index  $k$  (0 for pick, 1 for place) and a top-down view position, expressed as  $\mathbf{x}$ , i.e.,  $\mathbf{a}^t = (k^t, \mathbf{x}^t)$ . At each time step, the agent receives a reward  $r$  consisting of a dense reward component  $r^d$  and a sparse reward  $r^s$ .

## IV. FRAMEWORK: EXPLORLLM

### A. Observation and Action Spaces

Our methodology leverages the strengths of LLMs and VLMs to extract the observation space used for the RL framework, as depicted in Figure 2. LLMs reformulate user-provided language commands into predefined templates and highlight the objects within these templates to form an interpreted command vector  $\tilde{l}$ . For example, it identifies the pick object in a template like “Put [pick\_object] on the [place\_object].” It is important to note that, within a given task setting, the number and category of objects do not change. Utilizing VLMs as open-vocabulary object detectors, our system identifies and encloses objects relevant to the task within bounding boxes from the image in raw observation space  $\mathbf{o}^t$ , represented by their locations  $\mathbf{X}_{\text{vlm}} = [\mathbf{x}_{\text{vlm}_1}, \mathbf{x}_{\text{vlm}_2}, \dots]$ . RGB-D visual inputs are segmented into crops based on bounding box positions, denoted as  $\mathbf{M}_{\text{vlm}} = [\mathbf{m}_{\text{vlm}_1}, \mathbf{m}_{\text{vlm}_2}, \dots]$ . This method improves the system’s robustness to detection inaccuracies and varying object shapes. The interpreted commands  $\tilde{l}$ , the positional data  $\mathbf{X}_{\text{vlm}}$  and the image patches  $\mathbf{M}_{\text{vlm}}$  are then integrated into the reformulated RL observation  $\mathbf{s}^t$ .

As the VLM already extracts each object’s position  $\mathbf{X}_{\text{vlm}}^t[i^t]$ , the action space is converted into an object-centric residual action space, as shown in Figure 2. The reformulated action space consists of a primitive index  $k$ , an object index  $i$  and a residual position  $\mathbf{x}_{\text{res}}$ , expressed as  $\tilde{\mathbf{a}}^t = (k^t, i^t, \mathbf{x}_{\text{res}}^t)$ , where  $\mathbf{x}^t = \mathbf{X}_{\text{vlm}}^t[i^t] + \mathbf{x}_{\text{res}}^t$ . This residual action allows to pick or place objects at specific locations. This is, for example, needed when picking the letter O, and  $\mathbf{X}_{\text{vlm}}^t[i^t]$  denotes the center of the bounding box. In this case, the

---

**Algorithm 1** Exploration strategy  $\pi^E$ 

---

**Input:** state  $s^t$ , LLM policies  $\pi_H^{\text{LLM}}$ ,  $\pi_L^{\text{LLM}}$ **Parameter:** threshold  $\epsilon$ **Output:** action  $\tilde{a}^t$ 

- 1: Sample a random number  $j$  from  $U(0, 1)$
  - 2: **if**  $j \leq \epsilon$  **then**
  - 3: Run LLM-generated high level action policy  $\pi_H^{\text{LLM}}$   
 $\mathbf{a}_H^t = (k^t, i^t) = \pi_H^{\text{LLM}}(s^t)$
  - 4: Run LLM-generated low level action policy  $\pi_L^{\text{LLM}}$   
 $\mathbf{x}_{\text{res}}^t = \pi_L^{\text{LLM}}(s^t, \mathbf{a}_H^t)$   
 $\tilde{\mathbf{a}}^t = (k^t, i^t, \mathbf{x}_{\text{res}}^t)$
  - 5: **else**
  - 6: Run the reinforcement learning policy  $\pi^{\text{RL}}$   
 $\tilde{\mathbf{a}}^t = \pi^{\text{RL}}(s^t)$
  - 7: **end if**
  - 8: **return** action  $\tilde{\mathbf{a}}^t$
- 

residual action  $\mathbf{x}_{\text{res}}^t$  is needed to prevent picking the letter O at its empty center.

### B. LLM-Based Exploration

Traditional deep RL algorithms (e.g., SAC [22], PPO [23]) do not inherently promote frequent visits to high-value states in high-dimensional state-action spaces, making vision-based tabletop manipulation tasks particularly challenging. In such cases, RL agents may struggle when successful outcomes are rare. Leveraging the planning capabilities of LLMs and the perception strengths of VLMs can help guide the exploration process more effectively by tapping into the rich prior knowledge within these FMs. The LLM-based exploration strategy, denoted as  $\pi^E$  in Algorithm 1, draws inspiration from the  $\epsilon$ -greedy strategy. Specifically, during the rollout collection at each timestep, the off-policy RL agent employs the LLM-based exploration technique if a sampled random variable falls below the threshold  $\epsilon$ . Otherwise, the action is selected according to the current RL agent’s policy,  $\pi^{\text{RL}}$ , as detailed in Algorithm 1.

Prior research frequently prompts LLMs at every step to create plans for robotic manipulation, making the process highly resource-intensive. This method incurs significant time and financial costs due to the numerous LLM invocations required to train a single RL agent. Drawing inspiration from CaP [14], our methodology employs the LLM to hierarchically generate language model programs, which are then executed iteratively during the training phase as exploratory actions. The hierarchical language model programs include both high-level  $\pi_H^{\text{LLM}}$  and low-level  $\pi_L^{\text{LLM}}$  policy code programs. A high-level plan primarily involves selecting robot action primitives and the objects to interact with based on the current state of the robot and the objects.

In contrast to high-level tasks, instructing low-level actions poses a more significant challenge because high-level states and actions are more accessible and can be represented as language. When dealing with low-level actions, the complexity of the state becomes considerably more intricate, particularly for image-based problems. Therefore, instead

of a deterministic  $\pi$  code policy, we instruct the LLM to produce a code policy  $\pi_L^{\text{LLM}}$  for generating an affordance map according to the input image. The low-level exploration behavior is derived from a stochastic policy that relies on the values within this affordance map. Although the code generated by LLMs lacks guaranteed feasibility and accuracy in robot environments, these models can generate potentially useful policy candidates, with the one exhibiting the highest success rate being selected as shown in Figure 3.

## V. IMPLEMENTATION

The main components for the implementation of ExploR-LLM are RL agent, VLM-based object detection, and code policy generation by LLM.

1) *Reinforcement learning agent:* We use the Soft Actor-Critic (SAC) algorithms with modifications in the collecting rollout phase, detailed in Algorithm 1. Other implementation aspects remain consistent with the standard SAC approach in stable-baselines3 [24]. We employ two convolutional layers to transform every image patch into a vector  $\phi \in \mathbb{R}^{n \times d}$ , where  $n$  is the number of objects captured by VLM and  $d$  the dimension of each patch as encoded by the CNN. The vector is subsequently concatenated with the position, robot gripper state, and the extracted episodic language goal  $\tilde{l}$  to form a new vector  $\phi' \in \mathbb{R}^{n \times d'}$ , where  $d'$  denotes the dimension of each patch’s vector following encoding and concatenation. It then goes to a self-attention layer. The output features from this layer then go into a two-layer MLP. The aforementioned structure is consistently utilized across all actor and critic networks.

2) *VLM detection:* Utilizing an open-vocabulary object detector ViLD [25], objects in the environment can be identified by given specific labels. However, implementing this model online during training is time-consuming, so ViLD is utilized solely in the evaluation phase. In the training phase, the ground truth in the simulation is used to determine the center positions of the bounding boxes. It is important to note that ViLD’s position detection in real-world scenarios is not always flawless. To simulate this imperfection, noise following a Gaussian distribution with a standard deviation equivalent to half the radius of the image crop is applied to the ground truth positions.

3) *Code policy generation by LLM:* The policy code for executing high-level behavior is obtained using a few-shot prompt in GPT-4 [2]. It includes a list of available robot motion primitives to demonstrate the robot’s actions. A custom API is also provided to aid the LLM in reasoning, such as determining whether an object is held in the robot’s gripper or understanding the relationships between different objects. Following the approach demonstrated by [14], where LLMs have been shown capable of generating novel policy codes with example codes and commands, our prompt also includes examples. They are designed to guide the LLM in formulating plans and conducting geometric reasoning for our specific task scenarios.

For low-level exploration actions, we employ GPT-4 with Vision [2], which generates code using prompts that combine

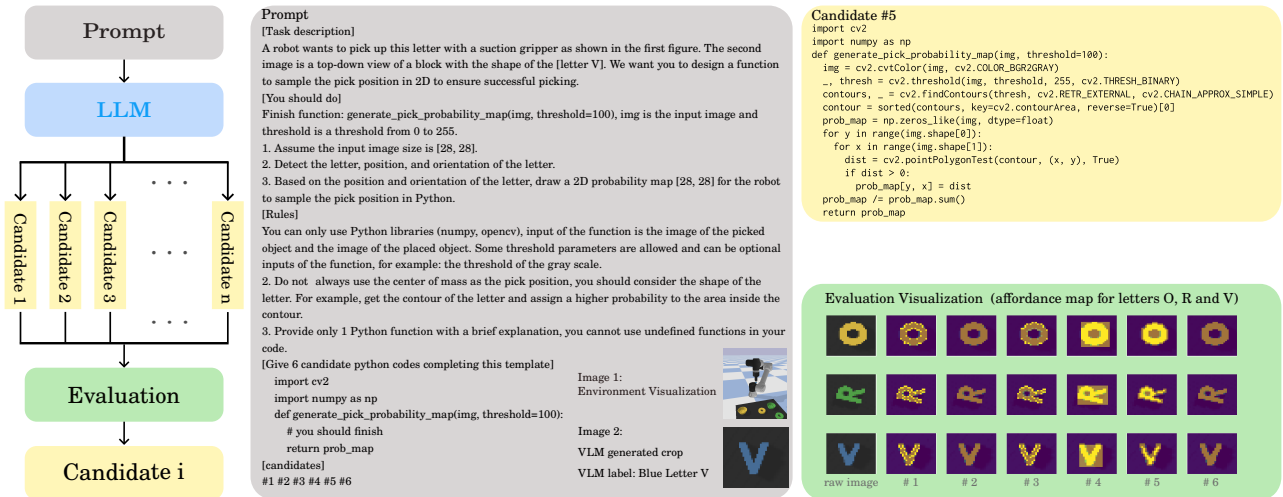


Fig. 3: Based on an exploration prompt, candidate policy code is generated. The exploration policy is selected after evaluation.

example images with language descriptions, enriching the context with visual information, as shown in Figure 3. The provided example images include a depiction of the environmental setup featuring the robot, a simulated background, objects, and a specific example of image patches inside VLM bounding boxes. The prompt describes the requirements and guidelines, enabling generated code to create a probability affordance heatmap for the specified image patch, utilizing external libraries like OpenCV and NumPy. However, as indicated in Figure 3, there are instances where the generated affordance map may not be optimal. For example, the optimal pick position for the letter O should be at its rim, whereas the heatmap suggests the center.

To address sub-optimality, we use a stochastic policy based on the affordance map instead of a deterministic one that selects the point of highest affordance. Since RL improves through rewards from environmental interactions, sub-optimal exploration policies can be corrected via learning. This approach also allows for the generation of counter-examples during replay buffer collection.

## VI. EXPERIMENTAL SETUPS

### A. Simulation Setup

The proposed method is trained and evaluated on a simulated tabletop pick-and-place task, as shown in Figure 2. Similar to [21] and [26], we use a UR5e, and the input observation is a top-down RGB-D image. Inspired by [26], we increased the task difficulty by replacing simple blocks with various objects, such as letters. We assess our method in two tasks: a short-horizon (SH) task, “Pick the [pick\_letter] and place it in the [place\_color] bowl”, and a long-horizon (LH) task, “Put all letters in the bowl of the corresponding color”, as shown in Figure 6a. In the SH task, each episode starts with three letters and three bowls randomly placed on the table, with pick-and-place actions generated from random language commands. The task is completed when the robot accurately places the chosen letter in the specified bowl. In the LH task, all letters and bowls are randomly arranged, and

the task is completed when each letter is placed in a bowl that matches its color.

### B. Real-World Setup

We validated our approach on a Franka Panda robot equipped with a suction gripper and an RGB-D camera, as shown in Figure 6a, implementing our policy and code in the EAGERx [27] framework. Given the potential risks to hardware and the time-intensive nature of direct training, we completed training in simulation, with real-robot applications limited to evaluation. We used ViLD for bounding box identification based on object names. To simulate real-world conditions more accurately, we introduced noise to the bounding box center’s position during the training phase in the simulation, mimicking the positional uncertainty inherent in VLM detection. We also added noise to bounding box positions and image inputs, simulating VLM detection uncertainty and camera noise, including lighting variations.

## VII. RESULTS

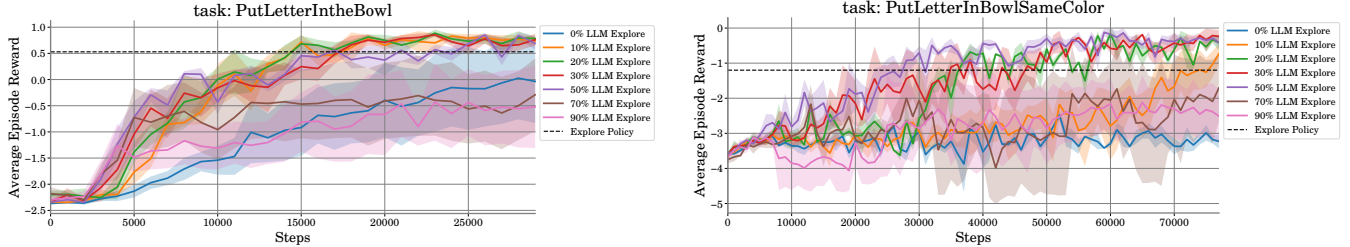
### A. Simulation Results

We investigated the effect of varying LLM-based exploration frequencies on training convergence, using  $\epsilon \in \{0.0, 0.1, \dots, 0.9\}$ , as shown in Figure 4. An  $\epsilon$  of 0 corresponds to standard SAC. Training was conducted with six random seeds per frequency, and each session began with a 20,000-step warm-up phase without LLM exploration, as no significant policy improvements were observed during this phase. Post-warm-up results, shown in Figure 4 and detailed in Table II for both short- and long-horizon tasks, indicate that ExploRLLM consistently outperforms LLM-only policies across various exploration frequencies.

In the short-horizon task (Figure 4a), training without LLM-based exploration is often unstable, resulting in either a successful policy or failure to converge. When the exploration frequency is within  $0 < \epsilon \leq 0.5$ , training stabilizes and converges more quickly, with minimal variation across different  $\epsilon$  values. However, increasing  $\epsilon$  beyond 0.5

TABLE I: Results of 50 evaluation episodes for short-horizon (SH), long-horizon (LH), and different initialization methods: no object overlap (NO) and allowed overlap (AO). ExploRLLM standard deviations are shown for 6 seeds.

Method	Overall success rate				Low-level error rate			
	SH NO	SH AO	LH NO	LH AO	SH NO	SH AO	LH NO	LH AO
ExploRLLM (20%)	0.86±0.05	0.80±0.06	0.70±0.11	0.54±0.09	0.14±0.05	0.20±0.06	0.18±0.10	0.22±0.09
ExploRLLM (0%)	0.56±0.40	0.48±0.36	–	–	0.32±0.24	0.42±0.30	–	–
CaP*	0.60	0.48	0.38	0.30	0.38	0.52	0.42	0.48
Socratic Models + CLIPort	0.78	0.64	0.50	0.36	0.22	0.28	0.22	0.28
Inner Monologue + CLIPort	0.82	0.72	0.58	0.42	0.18	0.26	0.20	0.24



(a) Pick the [pick letter] and place it in the [place color] bowl (SH).

(b) Put all letters in the bowl of the corresponding color (LH).

Fig. 4: Training curves for varying exploration rates in SH and LH tasks. ExploRLLM outperforms the exploration policies (dashed lines) and RL without LLM-based exploration ( $\epsilon = 0$ ). In the LH task, LLM-based exploration is crucial for success.

TABLE II: ExploRLLM training returns for varying  $\epsilon$ .

Explore $\epsilon$ (%)	SH Task (25k steps)	LH Task (75k steps)
0	-0.03 ± 1.13	-3.22 ± 0.29
10	0.74 ± 0.13	-0.73 ± 0.40
20	0.79 ± 0.06	-0.42 ± 0.31
30	0.76 ± 0.16	-0.23 ± 0.26
50	0.70 ± 0.17	-0.40 ± 0.23
70	-0.29 ± 0.98	-1.71 ± 1.38
90	-0.52 ± 1.12	-2.51 ± 1.09
Exploration Policy	0.53	-1.2

TABLE III: Success rate (%) of SH ExploRLLM with [4].

Task Settings	Seen	Unseen Color	Unseen Letters
Socratic Models + ExploRLLM	74	68	56
Socratic Models + CLIPort	72	50	34

reduces the proportion of online data, slowing progress and introducing greater instability into the training. For long-horizon tasks, Figure 4b shows that higher frequencies of LLM-based exploration ( $0 < \epsilon \leq 0.5$ ) correlate with faster training. These results highlight the importance of LLM-based exploration in navigating complex tasks by guiding experience toward the optimal region, mitigating challenges from large observation and action spaces. However, similar to the short-horizon tasks, excessive exploration rates introduce instability and slow convergence.

To evaluate the effectiveness of ExploRLLM, we benchmark its performance against four baselines: ExploRLLM without the LLM-based exploration policy, the CaP-style policy [14] (our exploration policy), Socratic Models [4], and Inner Monologue [12]. Our implementations of Socratic Models and Inner Monologue use ViLD [25] as the object detector and GPT-4 [2] as a multi-step planner. The individual steps are executed by a pre-trained CLIPort [26] model

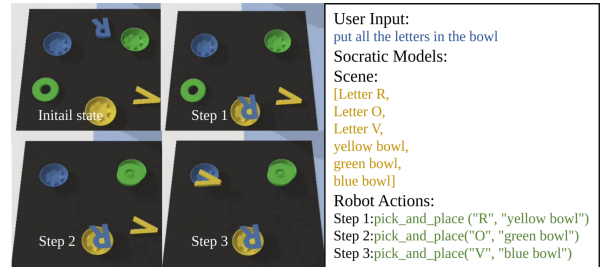


Fig. 5: Short-horizon ExploRLLM policies can be used in long-horizon tasks with zero-shot LLM planners, e.g. [4].

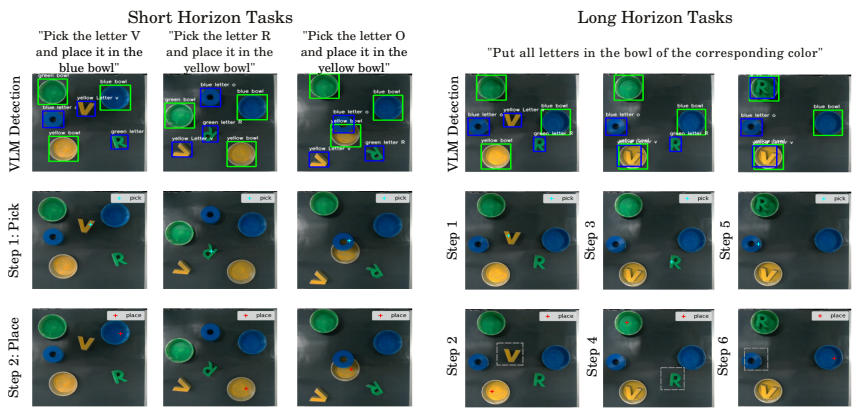
with 500 demonstrations. The key difference between Socratic Models and Inner Monologue is that Inner Monologue features a success detector that can identify mistakes.

During evaluation, the letter colors range from seen to unseen colors. Tasks and initialization methods vary, with “NO” indicating no overlap between the initial positions of letters and bowls, and “AO” allowing overlaps. These configurations assess each method’s robustness in handling complex object relationships.

For short-horizon tasks, as shown in Table I, ExploRLLM maintains stable performance, whereas versions without the exploration policy often fail to converge and exhibit high variance in success rates and low-level errors. Our method surpasses LLM-generated policies in success rates, reduces robot behavior errors, and minimizes the performance gap between NO and AO scenarios, emphasizing the exploration policy’s role in correcting FMs’ inaccuracies. In contrast, CLIPort-based methods struggle with novel scenarios or complex geometric object relationships. For long-horizon tasks, RL agents without LLM-based exploitation fail to converge. As shown in Table I, ExploRLLM outperforms Socratic Models, Inner Monologue, and LLM-generated poli-



(a) Real-world experimental setup.



(b) Visualization of VLM detections and pick and place actions.

Fig. 6: ExploRLLM can be practically applied using a sim-to-real approach with transfer due to VLM object detections.

cies, achieving superior results in long-horizon tasks.

Although our short-horizon agent is trained specifically for a pre-defined pick-and-place task, our approach can transfer to unseen long-horizon tasks in similar environments. This is made possible by integrating a zero-shot planner framework, such as Socratic Models [4]. This framework effectively breaks down user-provided input into individual action steps, each serving as a distinct language command for our single-step RL agent, as illustrated in Figure 5. Following the execution of each command, the task space is reset, allowing for the subsequent command to be executed. Apart from unseen colors, unseen letters are also included to evaluate the generalization capabilities of unseen scenarios. Table III demonstrates that the short-horizon ExploRLLM adapts to these settings, surpassing earlier Socratic Models versions. Using VLMs to provide bounding boxes and positions, our approach reformulates the observation space, enabling RL to focus on learning the physical attributes of objects, which is crucial for precise pick-and-place tasks. This strategy minimizes distractions from variations in colors and shapes.

### B. Real-World Results

We conducted real-world evaluations of ExploRLLM in two scenarios: one replicating all letters from the simulation experiments and another introducing the previously unseen letter ‘C’, with each scenario tested over 15 episodes. The short-horizon ExploRLLM achieved success rates of 66.6% for seen letters and 53.3% for the unseen letter scenario. In comparison, the long-horizon ExploRLLM recorded success rates of 40% for seen letters and 33.3% for unseen letters. Despite the Sim2Real gap, our approach shows promising results without additional real-world training. As the VLM extracts the observation space, the RL agent trained in simulation is less distracted by real-world noise. Figure 6b illustrates the adaptability of our method in handling diverse object orientations, understanding logical relationships between objects, and executing long-horizon tasks in real-world settings. However, challenges remain with noise in the color and depth perception of objects, which hampers the RL

agent’s ability to manipulate objects. Using a photorealistic simulator with extensive domain randomization is expected to improve performance.

### VIII. CONCLUSION AND DISCUSSION

In this work, we present ExploRLLM, a method that combines RL with FMs. By using actions informed by LLMs and VLMs to guide exploration, we accelerate RL convergence, demonstrating the benefits of integrating the strengths of both RL and FMs. We evaluated our method on tabletop manipulation tasks, showing superior success rates compared to policies based solely on LLMs and VLMs. ExploRLLM also generalizes to unseen colors, letters, and tasks. Ablation experiments with varying levels of LLM-guided exploration further highlighted its significant role in speeding up convergence. Additionally, we validated the method’s ability to transfer learned policies from simulation to real-world scenarios without additional training through real robot experiments. Currently, our framework focuses on tabletop manipulation, but we plan to extend it to a broader range of robotic manipulation tasks. While the system can correct low-level robotic actions, it struggles with mitigating high-level errors that are less frequent in simulations. Future work will focus on addressing these high-level discrepancies.

### REFERENCES

- [1] N. Di Palo, A. Byravan, L. Hasenclever, M. Wulfmeier, N. Heess, and M. Riedmiller, “Towards a unified agent with foundation models,” *arXiv preprint arXiv:2307.09668*, 2023.
- [2] OpenAI, “Gpt-4 technical report,” 2023.
- [3] W. Huang, P. Abbeel, D. Pathak, and I. Mordatch, “Language models as zero-shot planners: Extracting actionable knowledge for embodied agents,” in *International Conference on Machine Learning*. PMLR, 2022, pp. 9118–9147.
- [4] A. Zeng, M. Attarian, B. Ichter, K. Choromanski, A. Wong, S. Welker, F. Tombari, A. Purohit, M. Ryoo, V. Sindhwani *et al.*, “Socratic models: Composing zero-shot multimodal reasoning with language,” *arXiv preprint arXiv:2204.00598*, 2022.
- [5] W. Huang, C. Wang, R. Zhang, Y. Li, J. Wu, and L. Fei-Fei, “Voxposer: Composable 3d value maps for robotic manipulation with language models,” *arXiv preprint arXiv:2307.05973*, 2023.
- [6] T. Carta, C. Romac, T. Wolf, S. Lamprier, O. Sigaud, and P.-Y. Oudeyer, “Grounding large language models in interactive environments with online reinforcement learning,” *arXiv preprint arXiv:2302.02662*, 2023.

- [7] S. Kambhampati, K. Valmeekam, L. Guan, K. Stechly, M. Verma, S. Bhambri, L. Saldyt, and A. Murthy, "LLMs Can't Plan, But Can Help Planning in LLM-Modulo Frameworks," *arXiv preprint arXiv:2402.01817*, 2024.
- [8] J. Kober, J. A. Bagnell, and J. Peters, "Reinforcement learning in robotics: A survey," *The International Journal of Robotics Research*, vol. 32, no. 11, pp. 1238–1274, 2013.
- [9] R. S. Sutton and A. G. Barto, *Reinforcement learning: An introduction*. MIT press, 2018.
- [10] T. Kojima, S. S. Gu, M. Reid, Y. Matsuo, and Y. Iwasawa, "Large language models are zero-shot reasoners," *Advances in neural information processing systems*, vol. 35, pp. 22 199–22 213, 2022.
- [11] A. Brohan, Y. Chebotar, C. Finn, K. Hausman, A. Herzog, D. Ho, J. Ibarz, A. Irpan, E. Jang, R. Julian *et al.*, "Do as I can, not as I say: Grounding language in robotic affordances," in *Conference on Robot Learning*. PMLR, 2023, pp. 287–318.
- [12] W. Huang, F. Xia, T. Xiao, H. Chan, J. Liang, P. Florence, A. Zeng, J. Tompson, I. Mordatch, Y. Chebotar *et al.*, "Inner monologue: Embodied reasoning through planning with language models," *arXiv preprint arXiv:2207.05608*, 2022.
- [13] I. Singh, V. Blukis, A. Mousavian, A. Goyal, D. Xu, J. Tremblay, D. Fox, J. Thomason, and A. Garg, "ProgPrompt: Generating situated robot task plans using large language models," in *2023 IEEE International Conference on Robotics and Automation (ICRA)*. IEEE, 2023, pp. 11 523–11 530.
- [14] J. Liang, W. Huang, F. Xia, P. Xu, K. Hausman, B. Ichter, P. Florence, and A. Zeng, "Code as policies: Language model programs for embodied control," in *2023 IEEE International Conference on Robotics and Automation (ICRA)*. IEEE, 2023, pp. 9493–9500.
- [15] M. Kwon, S. M. Xie, K. Bullard, and D. Sadigh, "Reward design with language models," *arXiv preprint arXiv:2303.00001*, 2023.
- [16] W. Yu, N. Gileadi, C. Fu, S. Kirmani, K.-H. Lee, M. G. Arenas, H.-T. L. Chiang, T. Erez, L. Hasenclever, J. Humplik *et al.*, "Language to rewards for robotic skill synthesis," *arXiv preprint arXiv:2306.08647*, 2023.
- [17] J. Song, Z. Zhou, J. Liu, C. Fang, Z. Shu, and L. Ma, "Self-refined large language model as automated reward function designer for deep reinforcement learning in robotics," *arXiv preprint arXiv:2309.06687*, 2023.
- [18] Y. J. Ma, W. Liang, G. Wang, D.-A. Huang, O. Bastani, D. Jayaraman, Y. Zhu, L. Fan, and A. Anandkumar, "Eureka: Human-level reward design via coding large language models," *arXiv preprint arXiv:2310.12931*, 2023.
- [19] Y. Du, O. Watkins, Z. Wang, C. Colas, T. Darrell, P. Abbeel, A. Gupta, and J. Andreas, "Guiding pretraining in reinforcement learning with large language models," *arXiv preprint arXiv:2302.06692*, 2023.
- [20] E. Triantafyllidis, F. Christianos, and Z. Li, "Intrinsic language-guided exploration for complex long-horizon robotic manipulation tasks," *arXiv preprint arXiv:2309.16347*, 2023.
- [21] A. Zeng, P. Florence, J. Tompson, S. Welker, J. Chien, M. Attarian, T. Armstrong, I. Krasin, D. Duong, V. Sindhwani *et al.*, "Transporter networks: Rearranging the visual world for robotic manipulation," in *Conference on Robot Learning*. PMLR, 2021, pp. 726–747.
- [22] T. Haarnoja, A. Zhou, K. Hartikainen, G. Tucker, S. Ha, J. Tan, V. Kumar, H. Zhu, A. Gupta, P. Abbeel *et al.*, "Soft actor-critic algorithms and applications," *arXiv preprint arXiv:1812.05905*, 2018.
- [23] J. Schulman, F. Wolski, P. Dhariwal, A. Radford, and O. Klimov, "Proximal policy optimization algorithms," *arXiv preprint arXiv:1707.06347*, 2017.
- [24] A. Raffin, A. Hill, A. Gleave, A. Kanervisto, M. Ernestus, and N. Dormann, "Stable-baselines3: Reliable reinforcement learning implementations," *The Journal of Machine Learning Research*, vol. 22, no. 1, pp. 12 348–12 355, 2021.
- [25] X. Gu, T.-Y. Lin, W. Kuo, and Y. Cui, "Open-vocabulary object detection via vision and language knowledge distillation," *arXiv preprint arXiv:2104.13921*, 2021.
- [26] M. Shridhar, L. Manuelli, and D. Fox, "CLIPort: What and where pathways for robotic manipulation," in *Conference on Robot Learning*. PMLR, 2022, pp. 894–906.
- [27] B. van der Heijden, J. Luijkx, L. Ferranti, J. Kober, and R. Babuska, "Engine agnostic graph environments for robotics (eagerx): A graph-based framework for sim2real robot learning," *IEEE Robotics & Automation Magazine*, pp. 2–15, 2024.